UNIVERSITY OF CALIFORNIA SAN DIEGO

Anti-clogging Ventriculoperitoneal Shunt for Hydrocephalus

A Thesis submitted in partial satisfaction of the
requirements for the degree Master of Science

in

Engineering Science (Biomechanics and Biomedical Engineering)

by

Yau Ching Yun

Committee in charge:

Professor James Friend, Chair
Professor Clarie Scholtes Acevedo
Professor David Saintillan
Professor David Santiago-Dieppa

2024

The Thesis of Yau Ching Yun is approved, and it is acceptable in quality and form for publication on microfilm and electronically.

University of California San Diego

2024

DEDICATION

Dedicated to Professor James Friend and Dr. David Santiago Dieppa who are always there to provide support, encouragement, and always stand on my side.

EPIGRAPH

How much you can actually do is limited by the chemistry in your body,
but how much you want to achieve is limited by your desire and ambition.
-Yau C. Yun, 2024

I believe that ”the other me” exists in everyone’s heart.
It may be your ideal self that awaits you to reach it.
-Kazuki Takahashi, Yu-Gi-Oh! tankobon vol. 9

This is not guessing. This is a belief!
The belief that the response from your inner soul is the correct answer to the question.
The belief that you can influence the outcome.
Yau C. Yun, 2024

I am going to let him continue to evolve.
He will become the next generation of physicians.
Anonymous, 2022

TABLE OF CONTENTS

LIST OF FIGURES

ACKNOWLEDGEMENTS

I would like to acknowledge Professor James Friend for his support as the chair of my committee. His guidance and advice in both academic and life are invaluable. I really appreciate the weekly individual meeting. Without these long hours, the project would not reach this stage. I would also thanks Dr. David Santiago-Dieppa for his contribution to this project. Thank you for letting me scrub into the operating room for shadowing and thanks for allowing me to shadow and volunteer during clinic hours. Thank you for showing what is the meaning of being a great physician. I really appreciate that you believe in me in both my ability for this project and to become a future physician just like you. Minghao is also a vital member of this project. Thank you so much for helping me with my experiments. I appreciate how you are willing to stay late in the lab with me. I also want to thank Sujuith, Siyang, Lei, and Kha. Thank you for teaching me to use different equipment in the lab and for the advice for the experiment. I would also want to thank Aditya for allowing me to work on this project.

VITA

2023	B.S. in Mechanical Engineering, University of California, San Diego
2022	Grader, Department of Mechanical Engineering University of California, San Diego
2023	Lead Teaching Assistant, Department of Biological Science University of California, San Diego
2024	M.S in Engineering Science (Biomechanics and Biomedical Engineering), University of California, San Diego
2023	Undergraduate Researcher, Medical Advanced Devices Lab Advisor: James Friend, PhD
2024	Graduate Researcher, Medical Advanced Devices Lab Advisor: James Friend, PhD Co-Advisor: David Santiago-Dieppa, MD

FIELDS OF STUDY

Major Field: Engineering (Biomechanics and Biomedical Engineering)

Studies in Fluid Mechanics
Professors Xuanting Hao, Padmini Rangamani, and Andrew Cooper

Studies in Biomechanics
Professors David Saintillan, Claire Acevedo, and Stephanie Lindsey

ABSTRACT OF THE THESIS

Anti-clogging Ventriculoperitoneal Shunt for Hydrocephalus

by

Yau Ching Yun

Master of Science in Engineering Science (Biomechanics and Biomedical Engineering)

University of California San Diego, 2024

Professor James Friend, Chair

Hydrocephalus is a neurological disorder in which there is an excess accumulation of cerebrospinal fluid within the intracranial compartment that often results from cerebrospinal fluid flow obstruction. Patients with hydrocephalus experience headaches, a reduction in body coordination, an increase in sleepiness, blurred vision, hearing loss, and even loss of bladder control. Existing treatments include acetazolamide, and endoscopic third ventriculostomy, with ventriculoperitoneal (VP) shunt implantation being the existing golden standard. However, obstruction in the shunt system is a recurring issue after ventriculoperitoneal shunt implantation results in a need for shunt revision. Shunt implantation has medical expenditures of about one hundred-million-dollar with half of this amount subject to shunt revision. In our research, we

break the limit of shunt functionality by offering two novel approaches in fabricating the next-generation VP shunt system in addition to developing a new hydrocephalus experimental model. The first approach leverages the hyperelasticity of silicone to form a soft and flexible membrane to induce obstruction of the shunt via external saline injection. The second approach utilizes the characteristic of piezoelectric material, lithium niobate ($LiNbO_3$), to transduce ultrasound by applying input voltage at a specific frequency. The first approach was to recover the full flow rate after clogging in an experimental setting while the second approach can demonstrate the potential of unclogging after fabrication by showing its theoretical concept.

Chapter 1

Introduction

Hydrocephalus is a neurological disorder that results from an excess accumulation of cerebrospinal fluid. Cerebrospinal fluid (CSF) is a colorless fluid found within the intracranial compartment except the blood. CSF provides a variety of physiological functions such as serving as a shock absorber and immunological mechanism for the central nervous system (CNS). A typical approach in treating hydrocephalus requires an implant of a ventriculoperitoneal (VP) shunt system. The overall theme of this project anchors the introduction of the next-generation VP shunt system that solves the existing issues found in the current shunt system. Before the discussion of other aspects of hydrocephalus, an overview of the anatomy and physiology of the brain is first reviewed.

1.1 Anatomy, Physiology of the Brain and Hydrocephalus

The brain is part of the central nervous system along with the spinal cord. The brain can break down into multiple lobes (frontal, parietal, temporal, occipital) shown in **Figure 1.1**. Different lobes have different functions. The frontal lobe is located at the front of the brain and is responsible for higher-order cognitive functions such as problem-solving, emotion, motor function, speech formulation, and short-term memory. The temporal lobe is responsible for auditory information processing and language comprehension. The parietal lobe located on the upper back of the brain has the main function of sensory perception and integration such as

touch and temperature. Lastly, the occipital lobe is located on the back of the brain which is responsible for visual processing.

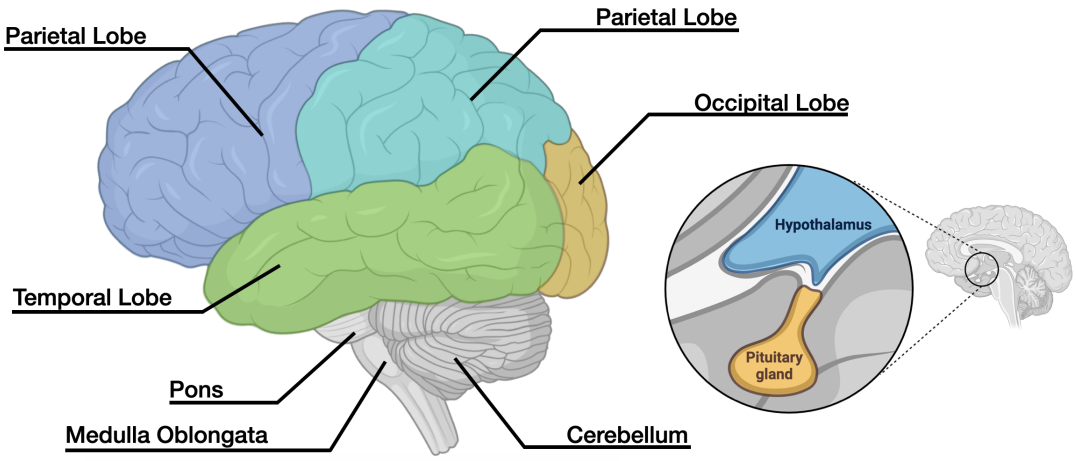

Figure 1.1. The four lobes within the human brain.

The pons are located below the temporal lobe and above the oblongata and have the main functions of signal relaying, and breathing control. Oblongata is responsible for a variety of involuntary controls such as swallowing, vomiting, blood pressure (BP), and also breathing. The cerebellum is responsible for movement coordination and balance. In the center region of the brain, there is the hypothalamus which has the function of maintaining physiological homeostasis such as body temperature regulation and hormone level. The pituitary gland is below the hypothalamus which is responsible for hormone secretion by receiving signals from the hypothalamus. The pituitary gland can further break down into posterior pituitary and anterior pituitary. The posterior pituitary serves as a reservoir that stores and secretes hypothalamic hormones while the anterior pituitary synthesizes and releases hormones in response to signals from the hypothalamus.

1.2 Ventricular System and Cerebrospinal Fluid

The entire ventricular system consists of four interconnected ventricles with two lateral ventricles, a third ventricle, and a fourth ventricle shown in **Figure 1.2**. The two lateral ventricles

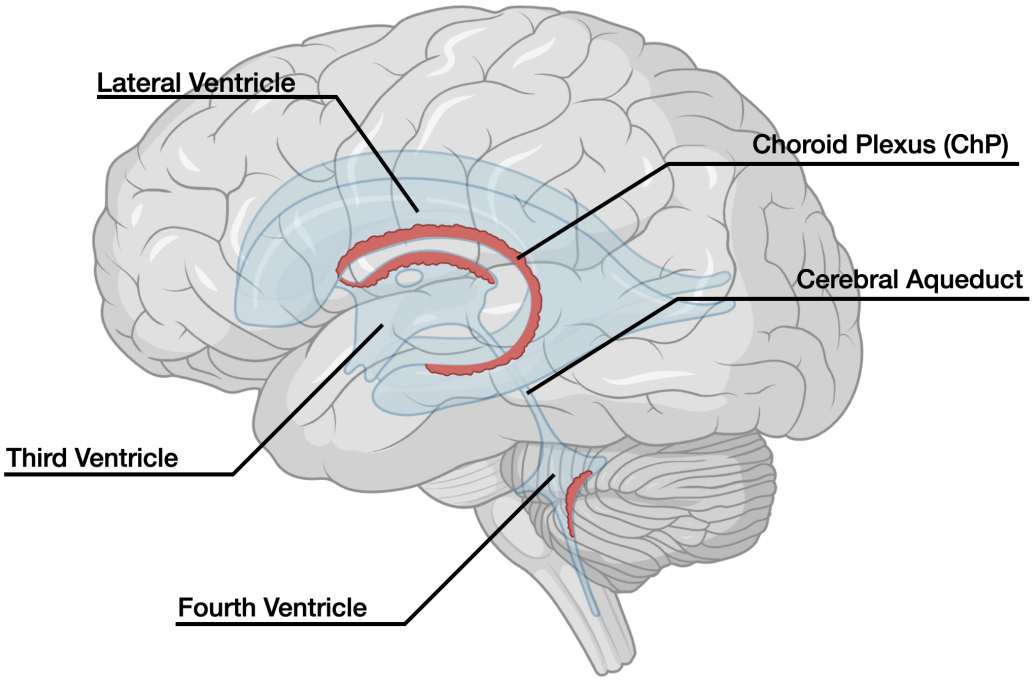

Figure 1.2. Brain structure focuses on the ventricle (light blue) and cerebrospinal fluid secretion site (red)

have a rough "C"-shape. The third ventricle is located in the center of the brain. The cerebral aqueduct allows CSF flow by bridging the third and the fourth ventricles [50]. The fourth ventricle is located near the brainstem and below the cerebellum. Each ventricle stores CSF and contains the structure, choroid plexus (ChP), on the wall, shown in **Figure 1.2**. The total CSF volume is 150 mL with all four ventricle occupied 40 mL [67]. The ChP is a structure on the ventricle wall that contains the epithelial tissue and its high surface area to volume ratio benefits its secretion of CSF into the ventricle [12, 68]. From the ventricles, CSF is then flow into the subarachnoid space which is sandwiched between the pia mater and the arachnoid membrane. Subarachnoid space serves as a buffer region that provides protection for the brain and the spinal cord.

The filtration of blood produces CSF which is secreted by the choroid plexus in the ventricle and attains a variety of physiological functions [29]. The function of cerebrospinal fluid includes the following.

(1) The buoyancy from the cerebrospinal fluid reduces pressure on nerves and blood vessels by reducing the weight of the brain.

(2) Cerebrospinal fluid works as a shock absorber by compressing the cerebrospinal fluid before the brain hits the skull [14].

(3) Blood-CSF Barrier (BCB): Regulation of extracellular environment by controlling the flux of electrolyte [63, 60, 70, 68, 11].

(4) Biomarker: Investigating CSF helps diagnosing neurological disorders [56, 70, 21]. For example, CSF is part of the diagnostic parameter for Alzheimer's disease [42].

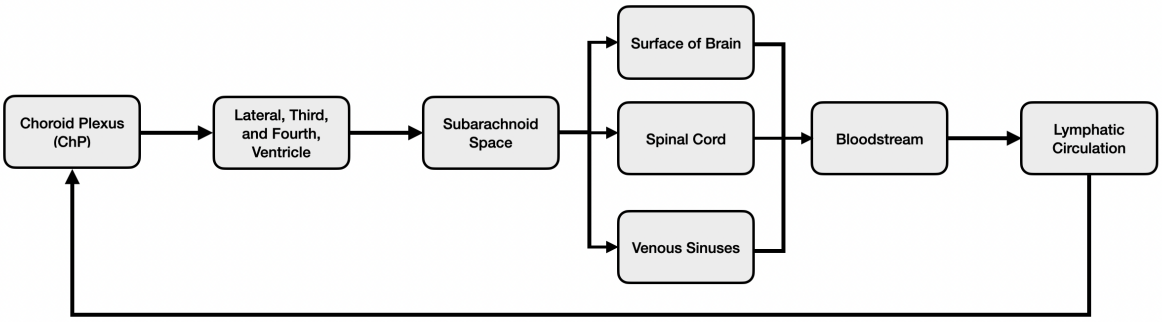

Figure 1.3. The simplified pathway for CSF circulation

The role of CSF plays a significant role in the brain. For humans, ChP has a variety of ion transporters that are needed to maintain ion homeostasis [68]. Choroid plexus establishes an osmotic gradient by pumping Na^+, K^+, $HCO_3{}^-$, other electrolytes, and other solutes such as vitamins out of the plasma into the ventricles [42, 48, 63]. The protein concentration in CSF is in fact less than 1% with 80% of proteins in CSF coming from blood [49]. Besides protein, CSF also contains various types of lipids such as phosphogylcerolipids and sphingolipids which correlate to CSF protein concentration [52]. The weight of the brain also reduces as a result of buoyancy from the cerebrospinal fluid. In humans, the net flow of CSF is about $0.4\,\mathrm{mL/min}\left(0.2-0.7\,\mathrm{mL/min}\right)$ which is about $600\,\mathrm{mL/day}$ [63, 58]. There are also different

techniques to monitor and track CSF. Magnetic resonance imaging (MRI) and the method of radioactive labeling are used to track CSF [63, 71]. The overall pathway of CSF secretion is shown in **Figure 1.3**; CSF is first secreted by the ChP which is located on the wall of the ventricle of the brain. Then, CSF flows from the lateral ventricles into the third ventricle and the fourth ventricle and finally reaches the subarachnoid space. In subarachnoid space, CSF begins to flow in different directions including the surface of the brain, spinal cord, intracranial venous sinuses, etc [66]. Finally, CSF will reach the bloodstream and be recycled by the lymphatic circulation [1].

Chapter 2

Neurological Procedure for Hydrocephalus and Existing Technology

2.1 Hydrocephalus

As described previously, hydrocephalus is a neurological disorder in which there is an excess accumulation of cerebrospinal fluid (CSF) within the intracranial compartment which often results from obstruction of CSF flow. The accumulation of CSF indicates the rate of CSF production is higher than the CSF reabsorption; this insufficient reabsorption results in hydrocephalus. Patients with hydrocephalus often experience headaches, poor body coordination, an increase in sleepiness, blurred vision, hearing loss, and even loss of bladder control [31, 54]. An average of 3 per 10000 infants experiences progressive hydrocephalus as a result of aqueductal stenosis (AS) [16]. Furthermore, patients subject to infections and shunt blockage also result in hydrocephalus [32]. Hydrocephalus can also be a complication after other diseases such as intraventricular hemorrhage (IVH) [8]. It can also result from complications of surgical procedures and tumors [51].

While hydrocephalus shows these general symptoms, there are various types of hydrocephalus. Hydrocephalus can be divided into two main types: (1) non-communicating (obstructive) hydrocephalus and (2) communicating (non-obstructive) hydrocephalus. Non-communicating hydrocephalus involves obstruction between ventricles which can reduce or inhibit the flow of CSF between the ventricles [9]. Symptoms of non-communicating hydro-

cephalus can cause a sudden elevation in intracranial pressure (ICP) which has the potential to induce sudden death [38]. Aqueductal stenosis is a common cause of non-communicating hydrocephalus. Other common causes of communicating hydrocephalus include congenital CNS malformations, tumors, meningitis that results in secondary obstruction, and fourth ventricle outlets obstruction [41]. As age increases, the chances of experiencing chronic hydrocephalus also increase. Chronic hydrocephalus falls into either one of the two categories. Chronic hydrocephalus occurs when there is a significant enlargement in the ventricle while the intracranial pressure (ICP) remains relatively stable [15]. Furthermore, normal hydrocephalus (NPH) occurs in all age groups with the elderly being the most common. NPH occurs when the increase in CSF build-up results in ventricles enlargement while the ICP remains constant and is classified as communicating hydrocephalus. NPH shares the subset of symptoms as hydrocephalus such as dementia, gait unsteadiness, and loss of bladder control [24]. Subarachnoid hemorrhage and head trauma can lead to NPH [13]. Besides studying the symptoms from clinical presentation, the diagnosis of all types of hydrocephalus typically involves an MRI or CT scan of the patient's head while MRI provides greater insights into the causes.

2.2 Pharmacological Intervention

Various types of oral medication are appropriate for treating hydrocephalus. Acetazolamide is a common medication that is a carbonic anhydrase inhibitor [65]. The ChP contains a high concentration of anhydrase cabon which catalyzes the conversion from CO_2 and H_2O to $HCO_3{}^-$. $HCO_3{}^-$ are tranported via NBCe2 protein channel into ventricle [10, 4]. Thus, inhibition of carbonic anhydrase inhibits the secretion of $HCO_3{}^-$ which reduces CSF secretion into the ventricle. Acetazolamide also reduces the expression of AQP1 which reduces the secretion of CSF [64, 3, 69, 65]. While it was not effective in children, good feedback is found in adults with hydrocephalus when the daily is within $200-500\,\text{mg}$ [55, 2]. Although pharmacological interventions are somewhat effective on adults, there exist side effects. For instance, paraesthesia,

dysgeusia, and an increase in tiredness are the general side effects that are dose-dependent [57].

2.3 Existing Treatment and Neurological Procedure

2.3.1 VP Shunt Approach and Existing Shunt System

The primary treatment of hydrocephalus involves the implantation of a ventriculoperitoneal (VP) shunt with about $36,000$ shunt implantation per year [6]. The neurosurgeon begins the procedure by first drilling a small hole in the patient's skull. The proximal catheter along with a rigid guide wire is then placed into the ventricle. The guide wire is then removed after the proximal catheter arrives at the required destination. The shunt is typically placed in the lateral ventricles but it can also be directed to the third or fourth ventricle in some circumstances. The proximal catheter is first connected to a valve which can control the flow rate of the CSF. A distal catheter is then connected to the other end of the valve which will redirect the CSF flow into the peritoneal cavity.

There are a variety of different shunt systems with a similar principle. For example, adjustable shunt and nonadjustable shunt. Adjustable shunt contains the valve component which can be *programmed* and thus regulate the fluid drainage. Some of the valves also can measure the pressure and flow [40]. There are also two types of valves including variable (adjustable) pressure valves and constant pressure valves. The strength of the variable pressure valve is that correction can be made after implantation. The pressure can be corrected via a magnet such that a magnetic field generates a magnetic torque to rotate the valve [62]. Adjustable shunt is found to be more expensive than nonadjustable shunt [59].

The main issue with the existing shunt is its durability; there is a high probability of experiencing malfunctions which is either underdrainage or overdrainage [36]. Underdrainage occurs when the rate of CSF removed from the ventricles is below the expected rate while overdrainage is the opposite of underdrainage. Overdrainage can lead to the collapse of the ventricle. The underdrainage is typically a result of shunt obstruction [39]. The current existing

VP shunt surgery is not perfect and often requires shunt revision due to obstruction. In the United States, medical expenditures for shunt implantation are about 100 million, with half of this amount subject to shunt revision [6]. From the UK Shunt Registry, the reported cumulative shunt revision rate is 24% and 14% within the first year, for children and adults respectively [43]. For a population of 1000 patients with a median age of around 41.6 years, the mean follow-up years is 9.2 years with 70% of the patients being adults [47]. Moreover, 54% of the patients require at least four shunt revisions and some patients also experience shunt infections [22]. Upon VP shunt implantation, there is an estimated infection rate of around 5% [27]. This indicates an evolution of the existing shunt system is needed as one of the main causes of the shunt revision is the result of clogging. A variety of techniques were used to evaluate shunt function which includes ultrasonography and MRI [5, 33]. Some cases of shun obstruction also include the growth of choroid plexus into the shunt [36].

Without any shunt revision, shunt obstruction can lead to serious consequences such as a rise in ICP which can trigger seizures, infection, and other symptoms associated with hydrocephalus. There are a few existing methods for alleviating this problem. CSF-infusions are one of the solutions for retrograde flush [43]. It starts with using two 25G butterfly needles with one needle recording the pressure and the second needle is responsible for infusion. Flow resistance and ICP are the parameters of interest to assess whether the infusion is completed or not [43]. Additionally, the recent development of shunt avoids traditional plastic tubes, instead, a composition of silicone and nitinol is used to fabricate the proximal catheter [16]. The benefit of this device is that it has the ability to change its size due to the property of nitinol wire while the silicone controls the initial geometry of the shunt [19, 44]. While Shunt is a preferred option under most circumstances. ETV is often an alternative in place of shunt revision as a result of shunt malfunction [23]. However, previous shunt insertion increases the surgical risk. Postoperative care is closely monitored.

While we discussed the basic principle of the existing shunt system, recent research attempts to develop the next-generation shunt that aims to the reducing clogging issue. Recent

development shows a catheter integrated with a backflow mechanism shows the capability to reduce blockage of shunt [45]. They suggest two approaches with one using a micropump to drive the backflow and the second approach using an electromagnetic backflow mechanism [45]. The micropump approach utilizes the flow generated from the micropump and drives back to the proximal end to induce unclogging. electromagnetic backflow mechanism utilizes a diaphragm that is sandwiched between an electromagnet and a metal to generate a backflow in order to induce unclogging by collapsing the metal plate onto the diaphragm due to electromagnetic force. In contrast to implementing additional components onto the shunt system, modification of the shunt geometry can also reduce clogging. Another research shows alternating the position of the ports on the shunt as a result of fluid dynamics optimization can also reduce clogging via computational fluid dynamics analysis [18].

2.3.2 Endoscopic Third Ventriculostomy (ETV) Approach

Endoscopic third ventriculostomy (ETV) is a minimally invasive procedure with the objective of restoring the homeostasis of CSF by creating an alternative circulation pathway in the third ventricle to the subarachnoid [61]. ETV is also a solution that often goes hand in hand with the VP Shunt implantation when there is shunt infection or shunt malfunctions [7]. ETV is an effective method for non-communicating hydrocephalus that is a result of structural abnormalities such as aqueductal stenosis [46]. The ETV procedure typically begins with creating a burr hole in the skull under anesthesia. An endoscope is inserted into the lateral ventricle and finally arrives at the third ventricle. The Fogarty catheter is then used to puncture the floor of the third ventricle thus creating an alternative pathway for CSF circulation. [53, 61]. A candidate for ETV shall show the signs of hydrocephalus, and the MRI shows the enlargement of the lateral and third ventricle relative to the regular size of the fourth ventricle [28]. It also requires the third ventricle to be sufficiently large to provide safe access for the endoscope without injuring the ventricle wall [28]. Comparing ETV and VP Shunt implantation, ETV is more suitable for non-communicating hydrocephalus has a shorter surgical time and hospital length of stay (LOS)

and there is a lower complication rate [9, 46]. Moreover, ETV is also proven to be safe and effective in children $(\text{mean age} = 6)$ [53]. While ETV is a suitable alternative to the VP shunt approach and attains a low complication rate, it is important to recognize its limitations. ETV is typically not suitable for patients with communicating hydrocephalus. Moreover, performing ETV increases the possibility of injuring nearby vessels that surround the ventricular system which can induce internal bleeding [34]. For example, a rupture of the basilar artery requires immediate abortion of ETV, and craniotomy is required. Although VP Shunt and ETV are great options treatment of hydrocephalus, lumber puncture serves as a short-term solution with a low post-operative infection rate [26].

Chapter 3

Next-Generation VP Shunt System

A recent study envisions the next generation VP shunt system which has the core objective to decrease the failure rate, lower shunt revision, and offer a variety of features including a communication system, ICP sensor, life-long battery, and other advanced features [37]. In this research, our objective is to deliver a next-generation shunt system with the ability to eliminate obstruction. In this research, we offer two novel approaches to the next-generation VP shunt system. The first approach takes advantage of the property of hyperelastic materials while the second approach utilizes acoustic wave streaming.

3.1 Soft Robotic Approach

3.1.1 Soft Robotic Shunt Design

As soft robotics is growing in the field of surgical devices, for instance, soft robotics was implemented into the steerable tip of the endovascular catheter [20]. In this design, we attempt to leverage the hyperelasticity of silicone as part of the components for the new shunt design. We modified the internal geometry of the shunt by increasing the inner diameter from a typical 1.5 mm to 2.770 mm while maintaining the standard outer diameter of 3.0 mm. The additional room allows the introduction of a silicone tube membrane (Ecoflex 30, Smooth-On, Macungie, PA USA) that is installed on the center of the shunt shown in **Figure: 3.1**. The material for the silicone membrane is Ecoflex 30, Smooth-On, Macungie, PA USA. The ports remain the

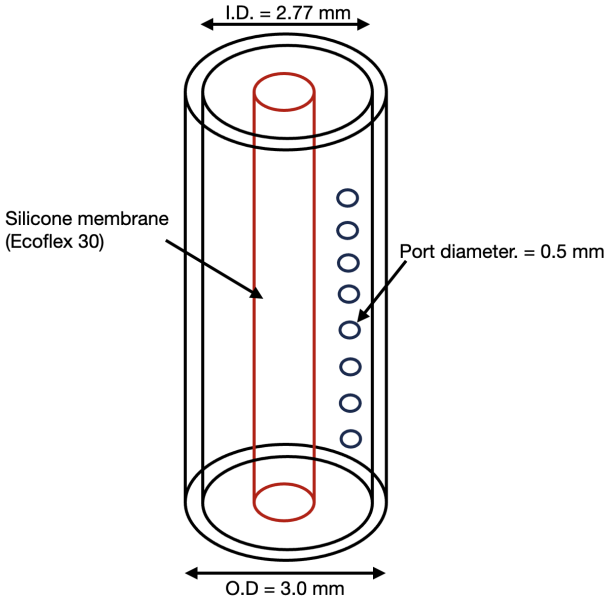

Figure 3.1. The general geometry of the shunt for the soft robotics approach. There are eight ports with 0.5 mm diameter aligned vertically for three sets separated by 120°. The red color tubes denote the silicone membrane.

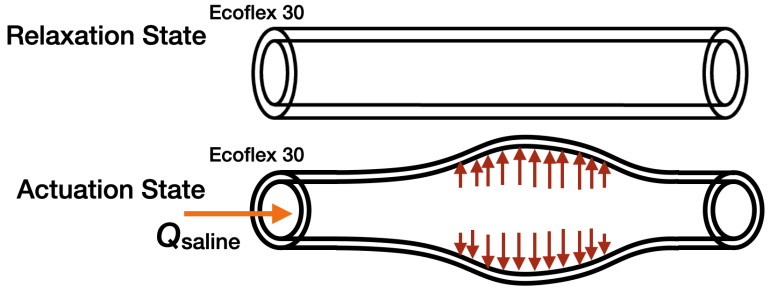

Figure 3.2. Shows the relaxation and actuation state of the silicone membrane.

same geometry with the standard 0.5 mm diameter. There are eight ports aligned vertically and this pattern is repeated every 120°. This device has two states, relaxation state and actuation state. During the relaxation stage, the Ecoflex 30 membrane is left as it is such that there is no deformation or changes in its geometry. During the actuation stage, a normal saline solution with 0.9% NaCl is pumped into the silicone membrane and this will expand shown in **Figure: 3.2**. During the experiment, the clogging agent will stick to the ports' region of the shunt. In order to remove the obstruction, the silicone membrane will be activated and change from a relaxation state to an actuation state via an injection of approximately 2 mL 0.9% NaCl solution. The

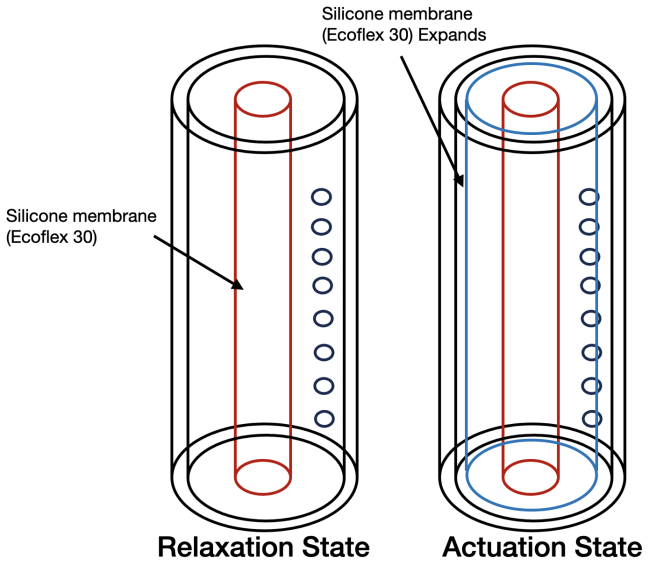

Figure 3.3. The general geometry of the shunt for the soft robotics approach. There are eight ports with 0.5 mm diameter aligned vertically for three sets separated by 120°. The red color tubes denote the Ecoflex 30 membrane. Blue denotes the membrane during the actuation state.

membrane inflates (actuation state) and this expansion pushes the clogging agent out of the port as a way to induce unclogging, shown in **Figure: 3.3**.

3.1.2 Fabrication Method

The fabrication of the proximal catheter of the VP shunt is a multi-step process. flow-governed layer casting process and peel-dominated demolding process have been used to fabricate a variety of geometry such as artificial blood vessels with high accuracy [17]. A similar technique has been used in our fabrication. The size of the membrane limits the geometry of the mold. A 1.1 mm diameter steel rod (uxcell) is used as the mold hollow cylinder geometry. An example of the setup of the mold is shown in **Figure: 3.4**.

The metal rod is aligned vertically and a mixture of part A and part B of the Ecoflex-30 is poured on top of the metal rod. The process is repeated for approximately 45 minutes until it is partially cured. After 24 hours, a thin layer of Ecoflex 30 membrane will be formed and can be removed from the metal rod with a tweezer.

The tip of the tubing is slightly larger than the diameter of the membrane as a result of

Figure 3.4. The mold setup for making the tubing

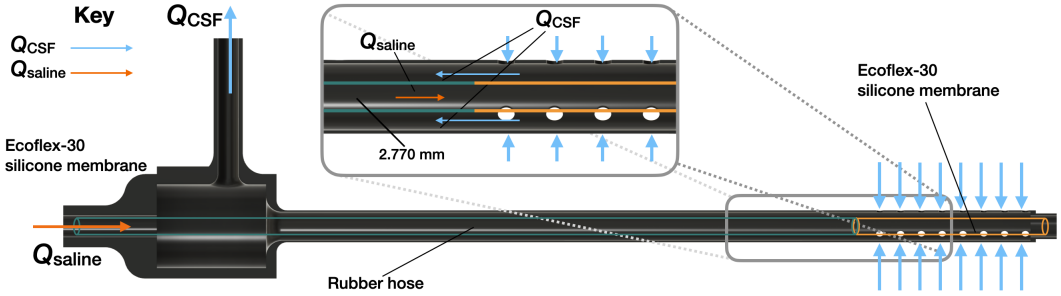

Figure 3.5. Shows the installation of the silicone membrane into the shunt

dripping due to gravity in this setup.

Our shunt for the soft robotic approach has two parts. The silicone membrane will first connected to the cap using UV glue. The cap along with the silicone membrane connects to the shunt shown in **Figure: 3.5** and **Figure: 3.6**

3.2 Acoustic Wave Streaming Approach

While the first approach utilized the hyperelasticity of silicone, the second approach utilized the vibration generated by the piezoelectric material when approaching a voltage at its resonance frequency. A transducer is first made and it is attached to the end of the shunt shown in **Figure: 3.7**. Wires connected from the power source will connected to the transducer. The transducer composed of three layers with a 0.5 mm thickness sandwiched between two 0.5 mm

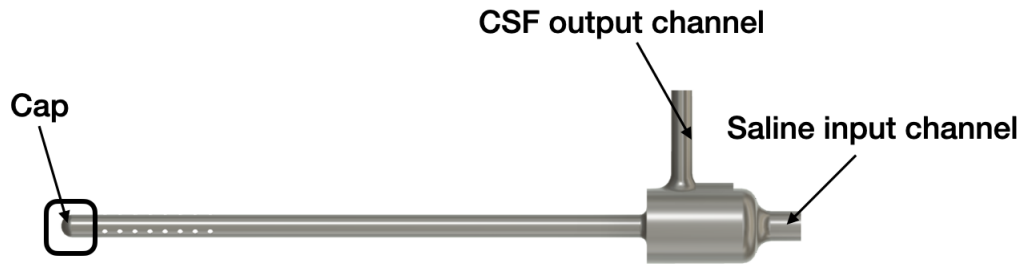

Figure 3.6. The CAD drawing of the shunt of all components attached

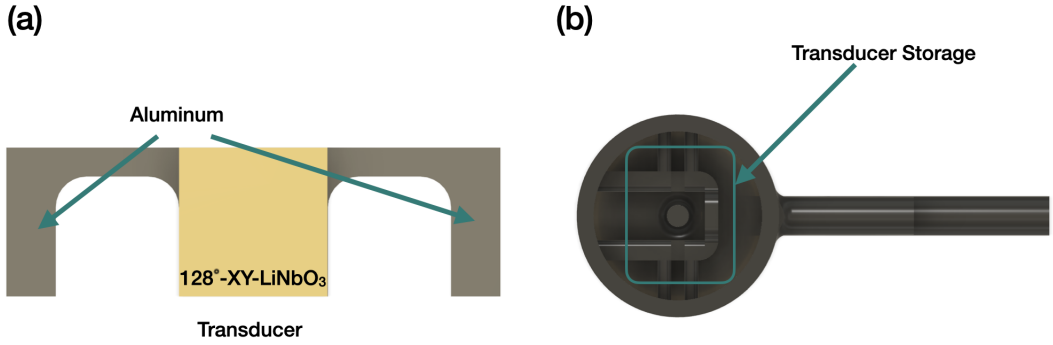

Figure 3.7. (a) Transducer architecture (Al-LN-Al) and (b) location of the transducer housing

128°-XY-$LiNbO_3$. As the shunt is being clogged, a voltage source is applied at its resonance frequency f_r. At f_r, the transducer is able to provide a large amplitude of wave propagation which can be induced unclogging due to vibration.

In order for the transducer to provide the most desired result, the dimension of the port size must match the wavelength of the wave propagation in water as a result of the transducer, shown in equation (3.1)

$$\lambda = 2\Phi \tag{3.1}$$

3.2.1 Determin the appropriate Geometry

The device is in thickness mode with the 128°-XY-$LiNbO_3$ sandwiched between two aluminum plates. The thickness of the 128°-XY-$LiNbO_3$ is set to be 0.5 mm. We decided to determine the appropriate thickness of the aluminum so that we can achieve the condition suggested in equation (3.1) because the thickness of 128°-XY-$LiNbO_3$ is more difficult to change.

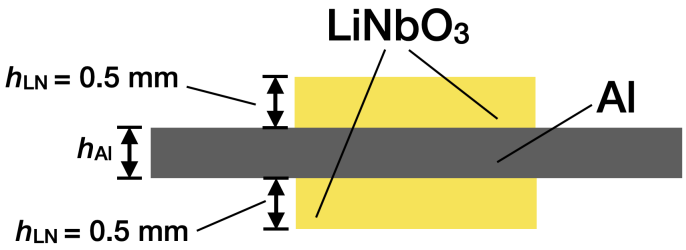

Figure 3.8. Shows the setup of the transducer which two 128°-XY-$LiNbO_3$ sandwich an aluminum plate with a thickness of h_{Al} to be determined.

The setup for eight transducers is shown in **Figure: 3.8**. The propagation velocity from the transducer can be approximated during the rule of mixture approximation

$$V_{\mathrm{TRD}} = \left(\frac{h_{\mathrm{Al}}}{h}\right) V_{\mathrm{Al}} + \left(\frac{h_{\mathrm{LN}}}{h}\right) V_{\mathrm{LN}} \tag{3.2}$$

$$h = h_{\mathrm{Al}} + 2h_{\mathrm{LN}} \tag{3.3}$$

where $h_{\mathrm{Al}}, h_{\mathrm{LN}}, h, V_{\mathrm{Al}},$ and h_{LN} are the thickness of the aluminum, thickness of 128°-XY-$LiNbO_3$, thickness of the structure, velocity of the wave on aluminum and the velocity of the wave on 128°-XY-$LiNbO_3$. Since $V_{\mathrm{TRD}} = \lambda \times f_r$ the frequency of the wave does not change as it passes from one medium to another. Hence, we have the following conditions,

$$\begin{cases} V_{\mathrm{TRD}} = 2h \times f_r = \left(\dfrac{h_{\mathrm{Al}}}{h}\right) V_{\mathrm{Al}} + \left(\dfrac{h_{\mathrm{LN}}}{h}\right) V_{\mathrm{LN}} \\ V_{\mathrm{H_2O}} = 2\Phi \times f_r \\ h = h_{\mathrm{Al}} + 2h_{\mathrm{LN}} \end{cases}$$

This method allows us to approximate the resonance frequency of the wave generated by the transducer. This helps us to validate whether the way see the measurement is correct or not.

The actual resonance frequency is determined experimentally with the ENA network analyzer (KEYSIGHT, San Diego, CA USA). The resonance frequency is 5.414 MHz while the 128°-XY-$LiNbO_3$ itself is around 6.9 MHz.

3.3 Clogging Agent

As previously described, the composition of CSF contains proteins and lipids. J. Larsen and G. Froning suggest utilizing IPA to solidify the egg yolk to allow easy separation of the egg yolk and vitelline [35]. Shell membrane, chalaza, and egg albumin are first separated from the egg. Vitelline is first then puncture and egg yolk spills out. A small amount of IPA is added to solidify the egg yolk. The albumin is then heated to $T = 100^{\circ}$ C for around 3 minutes to help solidify it while not denaturing it completely.

3.4 Experimental Model of Hydrocephalus

To assess the functionality of our innovations, an experimental model is needed. The physical setup is shown in **Figure: 3.9** and the schematic is shown in **Figure: 3.10**. We designed a fluidic system in which CSF analog, water is used in this case, flows from the open reservoir that is 30 cm above the centrifuge tube. The centrifuge tube represents the cerebral ventricle. From the cerebral ventricle, water flows down to the scale ventricle. The scale reservoir is sitting on the scale that has a load cell (HX711, Avia Semiconductor, Xiamen, P. R. China) which can sense the weight changes and report the mass value to the user's computer every five seconds. This experimental setup can determine the downstream pressure which is measured from the centrifuge tube to the scale reservoir. The height difference between the centrifuge tube to the scale reservoir is also 30 cm. The flow of water is driven by gravity which will become the source of pressure gradient.

The performance is evaluated by using the downstream pressure. This pressure can be determined using the analogous Ohm's Law.

$$\Delta p = Q_{\text{sys}} \times R \tag{3.4}$$

Where Q_{sys} is the systematic fluid rate of the circuit and R is the resistance generated from the

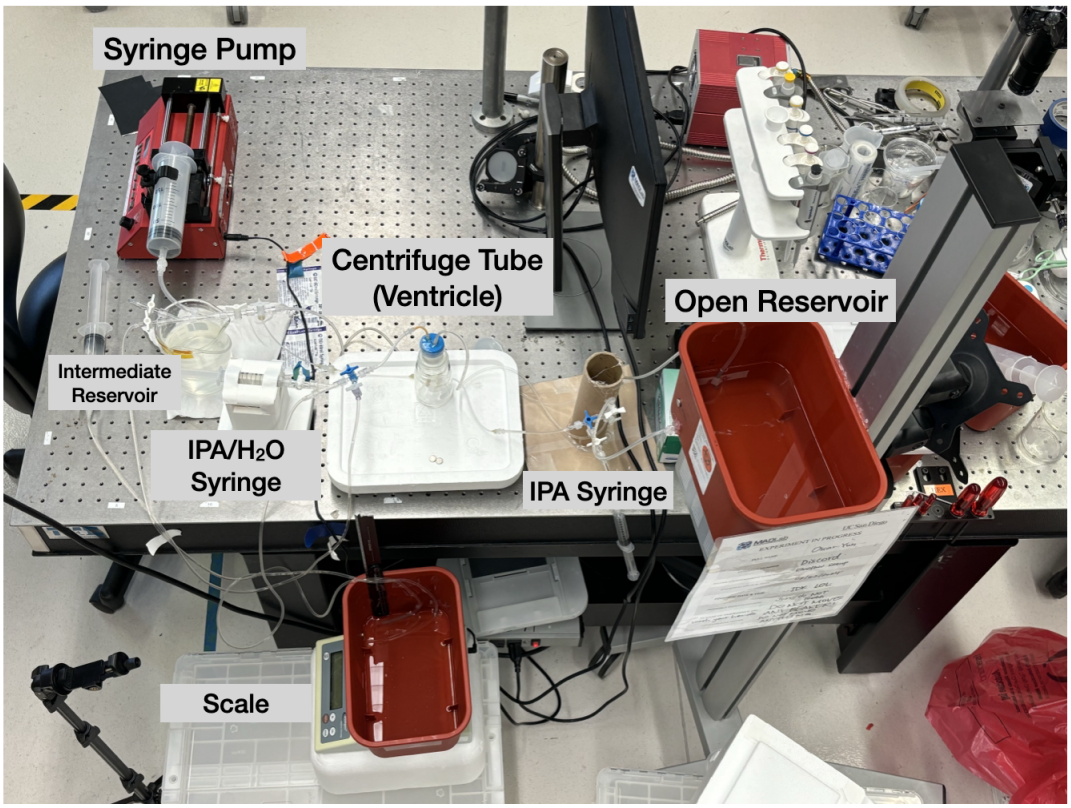

Figure 3.9. Image of the physical setup

tubes. The flow rate is low thus, we can safely assume the flow is laminar. We shall also assume steady state $(\partial/\partial t = 0)$, fully developed flow, $(\partial/\partial x = 0)$, axisymmetric flow, $(\partial/\partial \theta = 0)$. Using conservation of mass and conservation of momentum,

$$\partial_t \rho + \nabla(\rho \cdot \mathbf{u}) = 0 \tag{3.5}$$

$$\rho\left(\partial_t \mathbf{u} + \mathbf{u} \cdot \nabla \mathbf{u}\right) = -\nabla p + \mu \nabla^2 \mathbf{u} + \mathbf{f_b} \tag{3.6}$$

and the associated boundary condition and pressure profile,

$$u_x(r = \pm R) = 0 \tag{3.7}$$

$$|u_x(r = 0)| < \infty \tag{3.8}$$

$$\frac{\partial p}{\partial x} = -\gamma \tag{3.9}$$

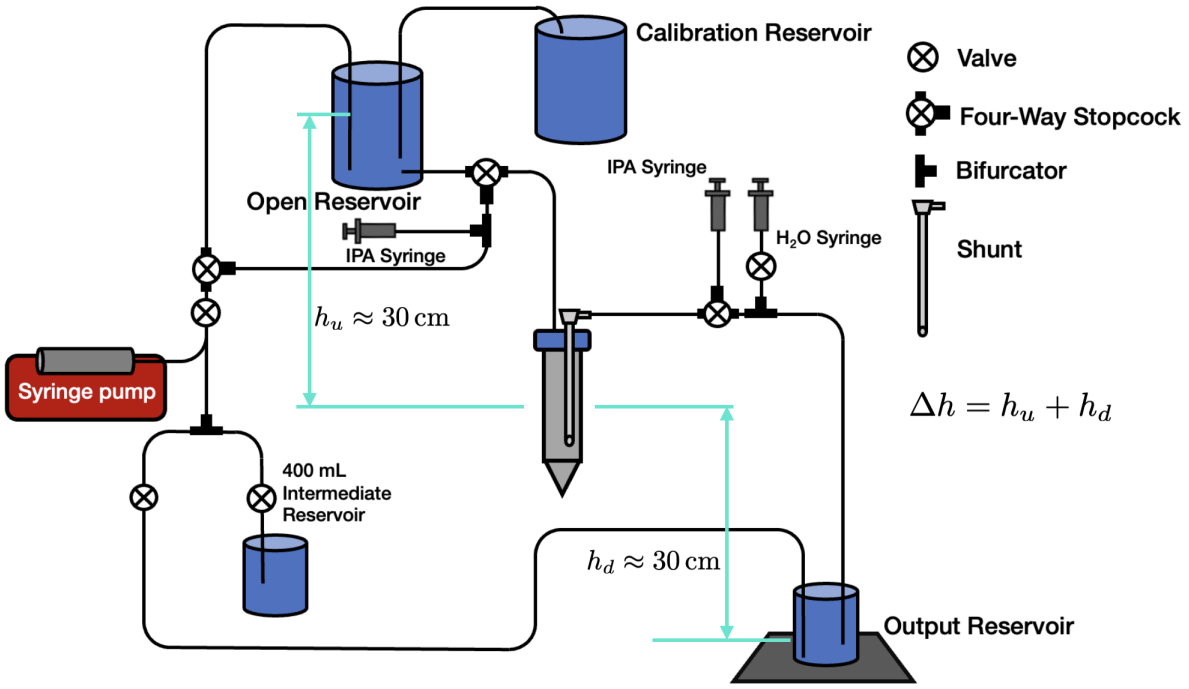

Figure 3.10. Schematic of the experimental setup for assessing shunt function

Where $\gamma = \rho g$, and this gives us,

$$Q = \left(\frac{\pi R^4}{8\mu L}\right)\gamma\Delta h \tag{3.10}$$

Hence, the resistance R is given by

$$R = \frac{8\pi\mu L}{A^2} \tag{3.11}$$

where A denotes the cross-sectional area of the tube. The downstream pressure is determined using the experiment flow rate and the downstream resistance. To find the experimental flow rate, we record the mass of CSF that enters the scale reservoir. Using the rate of change of the mass respective to time to determine the flow rate Q such that

$$Q(t_i) \approx \frac{1}{\rho\Delta t}\Big(m(t_i+\Delta t) - m(t_i)\Big) \quad \text{where } \Delta t = t_{i+1} - t_i \tag{3.12}$$

We need a model that describes the relationship between pressure p and flow rate Q. The schematic in **Figure: 3.10** can be converted into a circuit diagram shown in **Figure: 3.11**. This

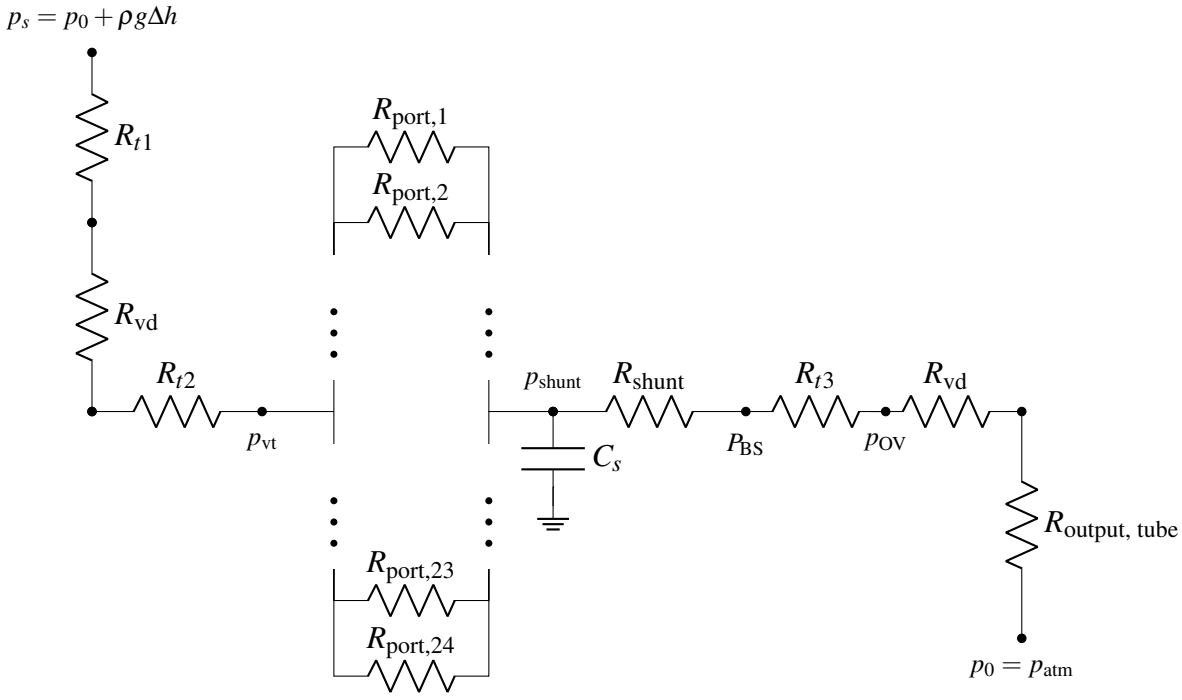

Figure 3.11. The circuit analogy of the fluidic circuit from schematic in **Figure: 3.10**

allows us to use an electrical analogy to determine the downstream resistance.

With p_s being the pressure on the open reservoir on the top shown in **Figure: 3.9**. p_{vt} is the pressure value inside the centrifuge tube relative to the scale reservoir. The resistance $R_{\text{port},i}$ is the resistance of the port and they are treated in parallel. Hence, the downstream pressure is

$$\Omega_d = R_{\text{port,eq}} + R_{\text{shunt}} + R_{\text{t3}} + R_{\text{t4}} + R_{\text{vd}} \tag{3.13}$$

where $R_{\text{port,eq}}$is equivalent to

$$R_{\text{port,eq}} \quad = \left(\frac{1}{R_{\text{port,1}}} + \frac{1}{R_{\text{port,2}}} + \frac{1}{R_{\text{port,3}}} + \frac{1}{R_{\text{port,23}}} + \frac{1}{R_{\text{port,24}}} \right)^{-1} \tag{3.14}$$

From here the theoretical equivalent resistance can be computed and thus, the theoretical flow rate can be derived.

$$Q^t_{\text{sys}} = \frac{\Delta p}{R^t_{\text{eq}}}. \tag{3.15}$$

The resistance from the valve cannot be determined using equation (3.11). Therefore, calibration is needed to determine the resistance from the valve on both the upstream R_{vu} and the downstream R_{vd}. R_d denotes the resistance downstream from the pressure p_{vt} while R_u denotes the resistance upstream from the pressure p_{vt} Therefore, we have the following relationship

$$R_d^e = R_d^t + R_{vd} \tag{3.16}$$

$$R_u^e = R_u^t + R_{vu} \tag{3.17}$$

R_u^e and R_d^e can be computed from the experimental flow rate and pressure. The pressure value is the same in both experimental and theoretical models. R_d^t and R_u^t are computed from the theoretical model. Hence, the value R_{vu} and R_{vd} can be found. The resistance value that used to compute p_{vt} is

$$\Omega_d = R_d^t + R_{vd} \tag{3.18}$$

Hence, the pressure $p_{\mathrm{d}}(t_i)$ is

$$p_d(t_i) = \frac{\Omega_d}{\rho \Delta t}\Big(m(t_i + \Delta t) - m(t_i)\Big) \tag{3.19}$$

The experiment consists of four setups. They are the positive control, control with clogging agent, soft robotic approach without clogging agent, and soft robotic approach with clogging agent. Both positive control and negative control are the existing Codman/tr shunt.

Chapter 4

Result and Discussion

4.1 Result

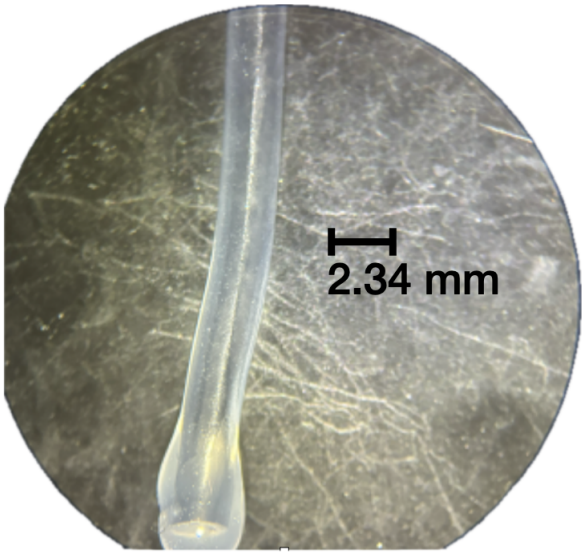

Figure 4.1. The result of the tubing and image is taken using iPhone 15 through a microscope.

A prototype of the shunt with a soft robotic device integration has been fabricated. The unclogging of the shunt has been demonstrated and video-recorded in an external environment. The image of the silicone tubing is shown in **Figure: 4.1**. The clogging agent which is composed of egg components is shown in **Figure: 4.3** With the current experimental setup, four sets of trials are completed. They are positive control, negative control, a soft robotic device without a clogging agent, and a soft robotic device with a clogging agent. **Figure 4.2** (a) shows the

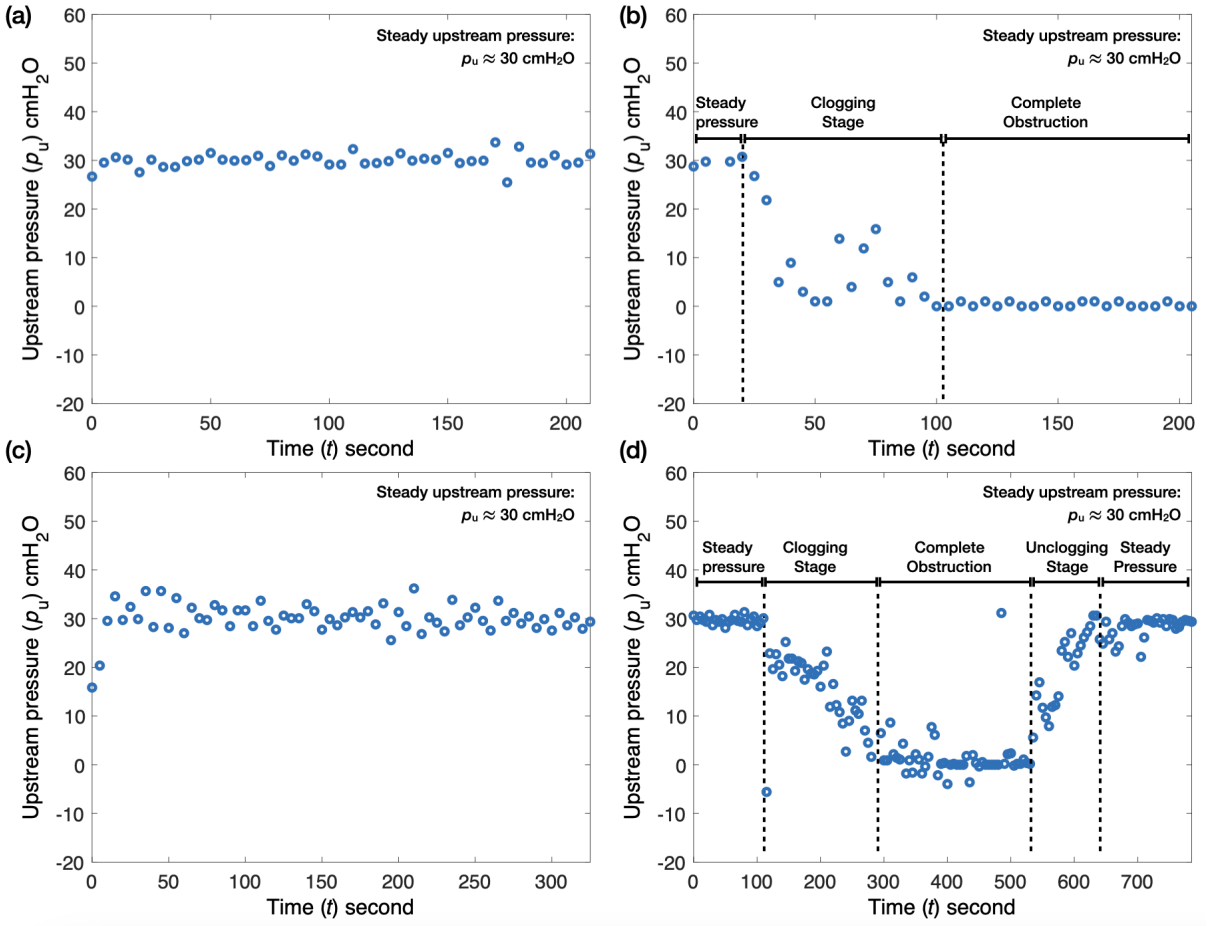

Figure 4.2. Shows the downstream pressure for (a) Codman®shunt with no clogging agent introduced,(b) Codman®shunt clogging agent introduced, (c) Soft robotic device with no clogging agent, (d) Soft robotic device integration with clogging agent.

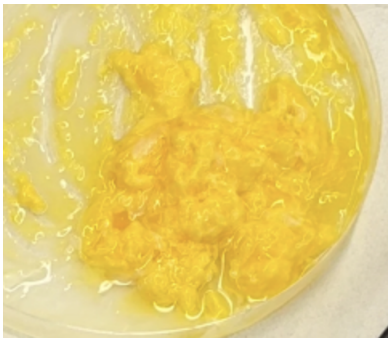

Figure 4.3. Shows the egg components that is extracted from the protocol described earlier.

VP shunt from Codamn® has a steady pressure profile of approximately 30 cmH$_2$O when no clogging agent is introduced. When the clogging agent is introduced shown in Figure **Figure 4.2**

(b), the downstream pressure decreases. The occlusion begins at approximately 25 seconds when rigorous shaking is applied. There is no flow recovery after the downstream pressure decreases to almost zero. Figure **Figure 4.2**(c) shows the pressure profile of the VP shunt with soft robotic device integration without a clogging agent. The downstream pressure remains near $30\,cmH_2O$. Figure **Figure 4.2** (d) shows the introduced VP shunt with soft robotic device integration with the clogging agent introduced. The downstream pressure is first remains at a steady pressure profile for around the first 100 seconds. Then, the centrifuge tube is shaken vigorously clogging being to form, and the downstream pressure drops. It eventually reaches almost zero downstream pressure. At this point, the soft robotic device is activated by water injection into that silicone membrane. The continuous injection and release induces unclogging. The downstream pressure increases eventually back to the steady state of $30\,cmH_2O$.

4.2 Discussion

This study focuses on the development of a next-generation VP shunt system that achieves the capability of removing obstruction of the clogged shunt. Traditional shunt serves as the golden standard for treating hydrocephalus [30]. However, the issue of shunt obstruction requires the patient to undergo another surgery for shunt revision which shunt revision contribute to almost of half of the medical cost for shunt surgery [6]. Therefore, the development of a new shunt is needed.

The silicone membrane is successfully fabricated and it is able to restore the downstream pressure as shown in **Figure 4.2** (d). Moreover, **Figure 4.2** (b) and (c) show the clogging agent clogged the shunt successfully. This is because the downstream pressure drops and eventually reaches a steady pressure of approximately $0\,cmH_2O$.

Figure 4.2 (b) shows that the existing shunt system does not have the ability to restore the downstream pressure. This results from the CSF analog cannot passes through the ports of the shunt. Thus, the rate change of the mass measured on the scale decreases. Reduction

in mass change reduces the downstream pressure. This is reflected in equation (3.19). The Codman®shunt does not have any additional biocompatible mechanism. There is no external force that can move the occluding agent while only the valve downstream can regulate the flow rate.

Results from **Figure 4.2** (a) and (c) show that our soft robotic device is able to main the same steady pressure at around $30\,\mathrm{cmH_2O}$. In contrast to the existing shunt device, our innovation can overcome this barrier as a result of the soft robotic integration. The inflation and deflation mechanism from the silicone membrane via water injection has the capability to unclog the VP shunt. This is reflected in the **Figure 4.2** (d). At time $t = 525$ s, the unclogging process begins. The silicone membrane turns from relaxation to actuation repetitively, the downstream pressure begins to increase. The removal of the occluding agent helps restore the flow rate which restores the downstream pressure. This rapid relaxation-actuation cycle helps push any clogging agent out of the ports. The return of the steady state pressure is comparable to the steady state without the clogging agent shown in **Figure 4.2** (c).

The fluctuation of these result is from the sensitivity of the strain gauge HX711 load cell. Any vibration can results in these fluctuation due to the HX711 load cell's sensitivity. This noise can also be seen by placing the scale reservoir on the load cell. Fortunately, the noise does not affect the reading of the steady, the processing of obstruction, and the pressure of unclogging. Since the pressure is obtained based on mass changes and recent work found the measuring mass using HX711 is reliable [25], therefore, the downstream pressure measurement is reliable.

While the soft robotic device is able to do unclogging, the limitation of the soft robotic device is limited by the silicone membrane. Any obstruction that is not in the port region, for instance, obstruction occurs in the distal end. The silicone membrane cannot reach a distance that is far away. As a result, the obstruction cannot be removed.

Bibliography

[1] Oluwaseun O Adigun and Mohammed A Al-Dhahir. Anatomy, head and neck, cerebrospinal fluid. 2017.

[2] G Aimard, A Vighetto, JY Gabet, P Bret, and E Henry. “Acetazolamide: an alternative to shunting in normal pressure hydrocephalus? Preliminary results”. In: Revue neurologique 146.6-7 (1990), pp. 437–439.

[3] Pouya A Ameli, Meenu Madan, Srinivasulu Chigurupati, Amin Yu, Sic L Chan, and Jogi V Pattisapu. “Effect of acetazolamide on aquaporin-1 and fluid flow in cultured choroid plexus”. In: Hydrocephalus: Selected Papers from the International Workshop in Crete, 2010. Springer. 2012, pp. 59–64.

[4] Dagne Barbuskaite, Eva K Oernbo, Jonathan H Wardman, Trine L Toft-Bertelsen, Eller Conti, Søren N Andreassen, Niklas J Gerkau, Christine R Rose, and Nanna MacAulay. “Acetazolamide modulates intracranial pressure directly by its action on the cerebrospinal fluid secretion apparatus”. In: Fluids and Barriers of the CNS 19.1 (2022), p. 53.

[5] AM Blitz, PP Huynh, LW Bonham, SK Gujar, DE Sorte, A Moghekar, MG Luciano, and D Rigamonti. “High-resolution MRI for evaluation of ventriculostomy tubes: assessment of positioning and proximal patency”. In: American Journal of Neuroradiology 41.1 (2020), pp. 57–63.

[6] Charles P Bondurant and David F Jimenez. “Epidemiology of cerebrospinal fluid shunting”. In: Pediatric neurosurgery 23.5 (1995), pp. 254–259

[7] Eva Brichtova, Martin Chlachula, Tomas Hrbac, and Radim Lipina. “Endoscopic third ventriculostomy in previously shunted children”. In: Minimally Invasive Surgery 2013 (2013).

[8] Yaoyao Bu, Meiyuan Chen, Ting Gao, Xiao Wang, Xuting Li, and Feng Gao. “Mechanisms of hydrocephalus after intraventricular haemorrhage in adults”. In: Stroke and Vascular Neurology 1.1 (2016), p. 23.

[9] HongWei Cheng, WenMing Hong, ZhaoJun Mei, and XiaoJie Wang. “Surgical management of non-communicating hydrocephalus in patients: meta-analysis and comparison of endoscopic third ventriculostomy and ventriculoperitoneal shunt”. In: Journal of Cranio- facial Surgery 26.2 (2015), pp. 481–486.

[10] Henriette L Christensen, Dagne Barbuskaite, Aleksandra Rojek, Hans Malte, Inga B Christensen, Annette C F ¨uchtbauer, Ernst-Martin F ¨uchtbauer, Tobias Wang, Jeppe Praetorius, and Helle H Damkier. “The choroid plexus sodium-bicarbonate cotransporter NBCe2regulates mouse cerebrospinal fluid pH”. In: The Journal of physiology 596.19 (2018), pp. 4709–4728.

[11] Oliver Cousins, Angela Hodges, Julia Schubert, Mattia Veronese, Federico Turkheimer, Jaleel Miyan, Britta Engelhardt, and Federico Roncaroli. “The blood–CSF–brain route of neurological disease: The indirect pathway into the brain”. In: Neuropathology and applied neurobiology 48.4 (2022), e12789

[12] Walter Edward Dandy. “Fluoroscopy of the cerebral ventricles”. In: The Journal of Nervous and Mental Disease 51.1 (1920), p. 63.

[13] Badih Daou, Petra Klinge, Stavropoula Tjoumakaris, Robert H Rosenwasser, and Pascal Jabbour. “Revisiting secondary normal pressure hydrocephalus: does it exist? A review”. In: Neurosurgical focus 41.3 (2016), E6.

[14] Lucien Diotalevi, Jean-Marc Mac-Thiong, and Yvan Petit. “Cerebrospinal Fluid Model Formulation Affects Global and Local Behaviour of the Spinal Cord Submitted to Transverse Traumatic Compression”. In: International Symposium on Computer Methods in Biomechanics and Biomedical Engineering. Springer. 2023, pp. 113–120.

[15] Richard J Edwards, Stephen M Dombrowski, Mark G Luciano, and Ian K Pople. “Chronic hydrocephalus in adults”. In: Brain pathology 14.3 (2004), pp. 325–336.

[16] Stephen P Emery, Stephanie Greene, Moataz Elsisy, Kaitlin Chung, Sang-Ho Ye, Seungil Kim, William R Wagner, Nika Hazen, and Youngjae Chun. “In vitro and in vivo assessment of a novel ultra-flexible ventriculoamniotic shunt for treating fetal hydrocephalus”. In: Journal of Biomaterials Applications 37.8 (2023), pp. 1423–1435.

[17] Dongliang Fan, Yuxuan Liao, Wenyu Wu, Ping Zhang, Xin Yang, Renjie Zhu, Yifei Wang, Canhui Yang, and Hongqiang Wang. “Flow casting soft shells with geometrical complexity and multifunctionality”. In: Advanced Materials Technologies 8.8 (2023), p. 2201640.

[18] Marcelo Galarza, A Gim ´enez, Jos ´e M Amig ´o, Martin Schuhmann, Roberto Gazzeri, U Thomale, and James P McAllister. “Next generation of ventricular catheters for hydrocephalus based on parametric designs”. In: Child’s Nervous System 34 (2018), pp. 267–
276.

[19] Hunter B Gilbert and Robert J Webster. “Rapid, reliable shape setting of superelastic nitinol for prototyping robots”. In: IEEE robotics and automation letters 1.1 (2015) pp. 98–105.

[20] Tilvawala Gopesh, Jessica H Wen, David Santiago-Dieppa, Bernard Yan, J Scott Pannell, Alexander Khalessi, Alexander Norbash, and James Friend. “Soft robotic steerable microcatheter for the endovascular treatment of cerebral disorders”. In: Science robotics 6.57 (2021), eabf0601.

[21] Catharina C Gross, Andreas Schulte-Mecklenbeck, Lohith Madireddy, Marc Pawlitzki, Christine Strippel, Saskia R ¨auber, Julia Kr ¨amer, Leoni Rolfes, Tobias Ruck, and Carolin Beuker. “Classification of neurological diseases using multi-dimensional CSF analysis”. In: Brain 144.9 (2021), pp. 2625–2634

[22] Nalin Gupta, Jeanna Park, Cynthia Solomon, Dory A Kranz, Margaret Wrensch, and Yvonne W Wu. “Long-term outcomes in patients with treated childhood hydrocephalus”. In: Journal of Neurosurgery: Pediatrics 106.5 (2007), pp. 334–339.

[23] Walter J Hader, Robin L Walker, S Terence Myles, and Mark Hamilton. “Complications of endoscopic third ventriculostomy in previously shunted patients”. In: Operative Neurosurgery 63.1 (2008), ONS168–ONS175.

[24] Salom ´on Hakim and Raymond D Adams. “The special clinical problem of symptomatic hydrocephalus with normal cerebrospinal fluid pressure: observations on cerebrospinal fluid hydrodynamics”. In: Journal of the neurological sciences 2.4 (1965), pp. 307–327.

[25] VOLODYMYR HAVRAN. “DETERMINING THE WEIGHT OF OIL EXTRACTED WITH A SCREW PRESS USING A STRAIN GAUGE SENSOR, HX711 MODULE, AND ARDUINO”. In: Herald of Khmelnytskyi National University. Technical sciences 331.1 (2024), pp. 73–76.

[26] A Heep, R Engelskirchen, A Holschneider, and P Groneck. “Primary intervention for posthemorrhagic hydrocephalus in very low birthweight infants by ventriculostomy”. In: Child’s Nervous System 17 (2001), pp. 47–51.

[27] Albert M Isaacs, Chad G Ball, Nicholas Sader, Sandeep Muram, David Ben-Israel, Geberth Urbaneja, Jarred Dronyk, Richard Holubkov, and Mark G Hamilton. “Reducing the risks of proximal and distal shunt failure in adult hydrocephalus: a shunt outcomes quality improvement study”. In: Journal of Neurosurgery 136.3 (2021), pp. 877–886.

[28] George I Jallo, Karl F Kothbauer, and I Rick Abbott. “Endoscopic third ventriculostomy”. In: Neurosurgical focus 19.6 (2005), pp. 1–4.

[29] Ahram Jang and Maria K Lehtinen. “Experimental approaches for manipulating choroid plexus epithelial cells”. In: Fluids and barriers of the CNS 19.1 (2022), p. 36.

[30] Farrukh Javeed, Anmol Mohan, Um Ul Wara, Lal Rehman, and Maham Khan. “Ventriculoperitoneal shunt surgery for hydrocephalus: one of the common neurosurgical procedures and its related problems”. In: Cureus 15.2 (2023).

[31] R Khazim, Z Dannawi, K Spacey, M Khazim, S Lennon, A Reda, and A Zaidan. “Incidence and treatment of delayed symptoms of CSF leak following lumbar spinal surgery”. In: European Spine Journal 24 (2015), pp. 2069–2076.

[32] Tommy Y Kim, Gail Stewart, Marcus Voth, James A Moynihan, and Lance Brown. “Signs and symptoms of cerebrospinal fluid shunt malfunction in the pediatric emergency department”. In: Pediatric emergency care 22.1 (2006), pp. 28–34.

[33] Kwok W Lam, James M Drake, and Richard SC Cobbold. “Noninvasive cerebrospinal fluid shunt flow measurement by Doppler ultrasound using ultrasonically excited bubbles: a feasibility study”. In: Ultrasound in medicine & biology 25.3 (1999), pp. 371–389.

[34] Jessica Lane and Syed Hassan A Akbari. “Failure of endoscopic third ventriculostomy”. In: Cureus 14.5 (2022).

[35] JE Larsen and GW Froning. “Extraction and processing of various components from egg yolk”. In: Poultry Science 60.1 (1981), pp. 160–167.

[36] Virginia Levrini, Zofia Czosnyka, Indu Lawes, Angelos G Kolias, and Richard Mannion. “Shunt Testing In Vivo: Illustration of Partially Obstructed Ventricular Catheter by In-Growing Choroid Plexus”. In: Cureus 12.7 (2020).

[37] Barry R Lutz, Pranav Venkataraman, and Samuel R Browd. “New and improved ways to treat hydrocephalus: pursuit of a smart shunt”. In: Surgical neurology international 4.Suppl 1 (2013), S38.

[38] Vijetha V Maller and Richard Ian Gray. “Noncommunicating hydrocephalus”. In: Seminars in Ultrasound, CT and MRI. Vol. 37. 2. Elsevier. 2016, pp. 109–119.

[39] Nadia Mansoor, Ole Solheim, Oddrun A Fredriksli, and Sasha Gulati. “Revision and complication rates in adult shunt surgery: a single-institution study”. In: Acta Neurochirurgica 163 (2021), pp. 447–454.

[40] Lina Momani, Abdel Rahman Alkharabsheh, and Waleed Al-Nuaimy. “Design of an intelligent and personalised shunting system for hydrocephalus”. In: 2008 30th Annual International Conference of the IEEE Engineering in Medicine and Biology Society. IEEE. 2008, pp. 779–782.

[41] Matic Munda, Peter Spazzapan, Roman Bosnjak, and Tomaz Velnar. “Endoscopic third ventriculostomy in obstructive hydrocephalus: A case report and analysis of operative technique”. In: World Journal of Clinical Cases 8.14 (2020), p. 3039.

[42] Cristina Municio, Laura Carrero, Desire ´e Antequera, and Eva Carro. “Choroid plexus aquaporins in CSF homeostasis and the glymphatic system: Their relevance for Alzheimer’s disease”. In: International Journal of Molecular Sciences 24.1 (2023), p. 878.

[43] Eva Nabbanja, John Douglas Pickard, Afroditi Despina Lalou, and Zofia Helena Czosnyka. “Use of CSF infusion studies to unblock occluded hydrocephalus ventricular shunt catheters: a preliminary report of two patients”. In: Case Reports 2018 (2018), bcr–2017.

[44] Gayani K Nandasiri, Anton Ianakiev, and Tilak Dias. “Hyperelastic properties of platinum cured silicones and its applications in active compression”. In: Polymers 12.1 (2020), p. 148.

[45] Anup Patel, David Qi, Jacqueline Boyle, Martin Morris, and Julian Lin. “Dual catheter and double-lumen cerebrospinal fluid shunt systems with backflow mechanisms”. In: Child’s Nervous System 40.1 (2024), pp. 135–143.

[46] Mohammad Rahman, Mohammad Salam, Kalim Uddin, Mohammad Islam, Mohammad Haque, Ahmed Hussain, and Mohammad Yusuf. “Early surgical outcome of endoscopic third ventriculostomy in the management of obstructive hydrocephalus: A randomized control trial”. In: Asian Journal of Neurosurgery 13.04 (2018), pp. 1001–1004.

[47] G Kesava Reddy, Papireddy Bollam, and Gloria Caldito. “Long-term outcomes of ventriculoperitoneal shunt surgery in patients with hydrocephalus”. In: World neurosurgery 81.2 (2014), pp. 404–410.

[48] Hansotto Reiber. “Flow rate of cerebrospinal fluid (CSF)—a concept common to normal blood-CSF barrier function and to dysfunction in neurological diseases”. In: Journal of the neurological sciences 122.2 (1994), pp. 189–203.

[49] Hansotto Reiber. “Proteins in cerebrospinal fluid and blood: barriers, CSF flow rate and source-related dynamics”. In: Restorative neurology and neuroscience 21.3-4 (2003), pp. 79–96.

[50] Jessica M Rubino and Jeffery P Hogg. “Neuroanatomy, cerebral aqueduct (Sylvian)”. In: (2019).

[51] Oumar Sacko, Sergio Boetto, Val ́erie Lauwers-Cances, Martin Dupuy, and Franck-Emmanuel Roux. “Endoscopic third ventriculostomy: outcome analysis in 368 procedures”. In: Journal of Neurosurgery: Pediatrics 5.1 (2010), pp. 68–74.

[52] Kosuke Saito, Kotaro Hattori, Shinsuke Hidese, Daimei Sasayama, Tomoko Miyakawa, Ryo Matsumura, Megumi Tatsumi, Yuuki Yokota, Miho Ota, and Hiroaki Hori. “Profiling of cerebrospinal fluid lipids and their relationship with plasma lipids in healthy humans”.In: Metabolites 11.5 (2021), p. 268.

[53] Arif Sarmast, Nayil Khursheed, Altaf Ramzan, Feroz Shaheen, Abrar Wani, Sarbjit Singh, Zulfikar Ali, and Bashir Dar. “Endoscopic third ventriculostomy in noncommunicating hydrocephalus: report on a short series of 53 children”. In: Asian Journal of Neurosurgery 14.01 (2019), pp. 35–40.

[54] David Satzer and Daniel J Guillaume. “Hearing loss in hydrocephalus: a review, with focus on mechanisms”. In: Neurosurgical review 39 (2016), pp. 13–25.

[55] Richard J Schain. “Carbonic anhydrase inhibitors in chronic infantile hydrocephalus”. In: American Journal of Diseases of Children 117.6 (1969), pp. 621–625.

[56] Lukas M Schilde, Steffen K ̈osters, Simone Steinbach, Karin Schork, Martin Eisenacher, Sara Galozzi, Michael Turewicz, Katalin Barkovits, Brit Mollenhauer, Katrin Marcus. “Protein variability in cerebrospinal fluid and its possible implications for neurological protein biomarker research”. In: PLoS One 13.11 (2018), e0206478.

[57] Christopher N Schmickl, Robert L Owens, Jeremy E Orr, Bradley A Edwards, and Atul Malhotra. “Side effects of acetazolamide: a systematic review and meta-analysis assessing overall risk and dose dependence”. In: BMJ open respiratory research 7.1 (2020), e000557.

[58] Dean A Seehusen, Mark M Reeves, and Demitri A Fomin. “Cerebrospinal fluid analysis”. In: American family physician 68.6 (2003), pp. 1103–1109.

[59] Yurdal Serarslan, Atilla Yilmaz, M ̈urteza C ̧akir, Ebru G ̈uzel, Akin Akakin, Aslan G ̈uzel, Boran Urfali, Mustafa Aras, Mustafa Emrah Kaya, and Nebi Yilmaz. “Use of programmable versus nonprogrammable shunts in the management of normal pressure hydrocephalus: A multicenter retrospective study with cost–benefit analysis in Turkey”. In: Medicine 96.39 (2017), e8185.

[60] Frederick B Shipley, Neil Dani, Huixin Xu, Christopher Deister, Jin Cui, Joshua P Head, Cameron Sadegh, Ryann M Fame, Morgan L Shannon, and Vanessa I Flores. “Tracking calcium dynamics and immune surveillance at the choroid plexus blood-cerebrospinal fluid interface”. In: Neuron 108.4 (2020), pp. 623–639.

[61] Paweł Sokal, Marcin Birski, Marcin Rusinek, Darek Paczkowski, Piotr Zieli ́nski, and Aleksandra Harat. “Endoscopic third ventriculostomy in treatment of hydrocephalus”. In: Videosurgery and Other Miniinvasive Techniques 7.4 (2012), pp. 280–285.

[62] Garrett J Soler, Mengdi Bao, Devina Jaiswal, Hitten P Zaveri, Michael L DiLuna, Ryan A Grant, and Kazunori Hoshino. “Focus: medical technology: a review of cerebral shunts, current technologies, and future endeavors”. In: The Yale Journal of Biology and Medicine 91.3 (2018), p. 313.

[63] Reynold Spector, S Robert Snodgrass, and Conrad E Johanson. “A balanced view of the cerebrospinal fluid composition and functions: Focus on adult humans”. In: Experimental neurology 273 (2015), pp. 57–68.

[64] Erik R Swenson. “Pharmacology of acute mountain sickness: old drugs and newer thinking”. In: Journal of Applied Physiology 120.2 (2016), pp. 204–215.

[65] Changwu Tan, Xiaoqiang Wang, Yuchang Wang, Chuansen Wang, Zhi Tang, Zhiping Zhang, Jingping Liu, and Gelei Xiao. “The pathogenesis based on the glymphatic system, diagnosis, and treatment of idiopathic normal pressure hydrocephalus”. In: Clinical Interventions in Aging (2021), pp. 139–153.

[66] Lauren N Telano and Stephen Baker. “Physiology, cerebral spinal fluid”. In: (2018).

[67] Ahmed Toma. “Hydrocephalus in adults”. In: Principles of Neurological Surgery. Elsevier, 2018, pp. 822–831.

[68] Masaki Ueno, Yoichi Chiba, Ryuta Murakami, Yumi Miyai, Koichi Matsumoto, Keiji Wakamatsu, Toshitaka Nakagawa, Genta Takebayashi, Naoya Uemura, and Ken Yanase. “Transporters, Ion Channels, and Junctional Proteins in Choroid Plexus Epithelial Cells”. In: Biomedicines 12.4 (2024), p. 708.

[69] Gonzalo Vilas, Devishree Krishnan, Sampath Kumar Loganathan, Darpan Malhotra, Lei Liu, Megan Rachele Beggs, Patrizia Gena, Giuseppe Calamita, Martin Jung, and Richard Zimmermann. “Increased water flux induced by an aquaporin-1/carbonic anhydrase II interaction”. In: Molecular Biology of the Cell 26.6 (2015), pp. 1106–1118.

[70] Junhua Xie, Arnout Bruggeman, Clint De Nolf, Charysse Vandendriessche, Griet Van Imschoot, Elien Van Wonterghem, Lars Vereecke, and Roosmarijn E Vandenbroucke. “Gut microbiota regulates blood-cerebrospinal fluid barrier function and Aβ pathology”. In: The EMBO Journal 42.17 (2023), e111515.

[71] Shinya Yamada. “Cerebrospinal fluid physiology: visualization of cerebrospinal fluid dynamics using the magnetic resonance imaging Time-Spatial Inversion Pulse method”. In: Croatian medical journal 55.4 (2014), pp. 337–346.